scientific reports

Check for updates

OPEN

From discovery to potential application: engineering a novel M23 peptidase to combat *Listeria monocytogenes*

Magdalena Kaus-Drobek[1]✉, Marzena Nowacka[1], Magdalena Gewartowska[2], Małgorzata Korzeniowska nee Wiweger[1], Merete Rusås Jensen[3], Trond Møretrø[3], Even Heir[3], Elżbieta Nowak[4,5] & Izabela Sabała[1]✉

Peptidoglycan hydrolases are promising alternatives for combating pathogens due to their specificity and potent bacteriolytic activity. In this study, a novel M23 peptidase from *Streptococcus thermophilus* NCTC10353, designated StM23, was discovered and characterized. It exhibited antibacterial activity against *Listeria monocytogenes* and other Gram-positive bacteria with *meso*-DAP-type peptidoglycan, including *Bacillus subtilis* and *Bacillus cereus*. To enhance StM23's efficacy and specificity, a chimeric enzyme, StM23_CWT, was engineered by fusing its catalytic domain with a cell wall-targeting domain (CWT) from SpM23B, a peptidoglycan hydrolase found in *Staphylococcus pettenkoferi*. The engineered chimera demonstrated expanded specificity, showing activity against *Staphylococcus aureus* and *Enterococcus faecium*. Its ability to disrupt *L. monocytogenes* cells was visualized by electron microscopy. The enzyme effectively disrupted biofilm structures and decontaminated surfaces like glass, stainless steel, and silicone, showcasing its industrial potential. Safety evaluations using zebrafish, moth larvae, and human cell models confirmed its non-toxic profile, supporting its broad applicability. Based on these findings, StM23_CWT is a novel and potent antimicrobial agent with significant potential to reduce the risk of listeriosis and control persistent pathogens.

Keywords M23 peptidases, Peptidoglycan hydrolases, *Listeria monocytogenes*, Biofilm eradication, Antimicrobial agents

Listeria monocytogenes is the causative agent of listeriosis, a severe infection that can lead to meningitis, septicaemia, and even death, particularly in immunocompromised individuals, pregnant women, and the elderly[1]. Listeriosis outbreaks are primarily linked to the consumption of contaminated RTE foods, including deli meats, soft cheeses, smoked fish, and pre-packaged salads. The ability of *L. monocytogenes* to persist in food processing environments complicates its control, posing a continuous risk for cross-contamination with other bacteria during food production and packaging[2]. Traditional approaches to controlling *L. monocytogenes* in food processing environments, such as chemical sanitizers and heat treatments, face certain limitations, including the emergence of resistant strains and potential negative impacts on food quality and safety[3–6]. Additionally, their effectiveness against biofilm structures formed on various surfaces in food production settings remains a significant challenge[7,8]. Thus, listeriosis outbreaks with severe consequences are reported each year and with the number of confirmed listeriosis cases reported to increase in the European Union/European Economic Area[9]. Importantly, standard antibiotic treatments of infected individuals are becoming less effective due to the rise of antibiotic-resistant strains and concerns about their effects on the microbiome[3,10,11]. Therefore, there is a pressing need for novel and more targeted approaches not only for listeriosis treatment but especially to mitigate the risk of *L. monocytogenes* in RTE foods.

[1]Laboratory of Protein Engineering, Mossakowski Medical Research Institute, Polish Academy of Sciences, Pawinskiego 5, 02-106 Warsaw, Poland. [2]Electron Microscopy Research Unit, Mossakowski Medical Research Institute, Polish Academy of Sciences, Pawinskiego 5, 02-106 Warsaw, Poland. [3]Nofima, Norwegian Institute for Food, Fisheries and Aquaculture Research, P.O. Box 210, 1431 Ås, Norway. [4]Laboratory of Protein Structure, International Institute of Molecular and Cell Biology, Trojdena 4, 02-109 Warsaw, Poland. [5]Preclinical Drug Development Facility, International Institute of Molecular and Cell Biology, Trojdena 4, 02-109 Warsaw, Poland. ✉email: mdrobek@imdik.pan.pl; isabala@imdik.pan.pl

In recent years, lactic acid bacteria (LAB), cocktails of phages and bacteriolytic enzymes either produced by bacteriophages (endolysins) or by bacteria (autolysins and bacteriocins) have emerged as promising alternatives for controlling *L. monocytogenes*[12]. The bacteriolytic enzymes are peptidoglycan hydrolases (PGHs) that degrade the bacterial cell wall, leading to rapid lysis of the target bacteria. Unlike traditional antibiotics, peptidoglycan hydrolases exhibit well defined specificity, that can be limited to particular species, reducing the likelihood of off-target effects on beneficial microflora. Moreover, peptidoglycan hydrolases have demonstrated efficacy against antibiotic-resistant strains, making them a powerful tool in combating foodborne pathogens[13]. PGHs are a diverse group of enzymes characterized by their ability to break down specific bonds within the peptidoglycan matrix, a crucial component of bacterial cell walls. They have multidomain architecture and are composed of at least one enzymatically active domain (EAD) usually accompanied by cell wall targeting domain(s) (CWT). Depending on the type of EAD, PGHs can function as glycosidases that cleave glycosidic bonds, amidases that target amide bonds, or peptidases that break peptide bonds. They can possess two active catalytic units, which boost their potency and efficiency while reducing the risk of resistance development. The cell wall targeting domains (CWTs) enhance the enzyme's lytic activity by guiding it to specific components of the bacterial cell wall. This combination of catalytic action and targeted specificity makes PGHs essential for degrading bacterial cell walls and holds promise for antibacterial applications[14]. The modular structure of PGHs provides an excellent framework for the development of novel and enhanced variants that exhibit improved lytic activity and stability. Several studies have demonstrated the effectiveness of strategies such as domain fusions, swapping, deletions, and linker modifications[15,16]. A widely used approach for improving enzyme performance involves creating chimeric enzymes by combining known catalytic domains with different cell wall targeting domains. The CWT domains include LysM, various subtypes of the SH3 domain, cell wall binding domains (CBDs) from listerial endolysins, and others[15]. The activity of PGHs can often be influenced by environmental conditions such as pH, temperature, and ionic strength and buffer components. As a result, much of the focus in protein engineering is directed at improving enzyme performance under a wide range of conditions. One prominent example of this is the M23 catalytic domain of LytM from *Staphylococcus aureus*, which, when combined with the SH3b domain from lysostaphin (Lss), exhibited significantly higher activity and expanded tolerance to high ionic strength and varying pH levels[17]. A similar approach was applied to EnpA, where fusion with different SH3b domains from lysostaphin, SpM23B from *Staphylococcus pettenkoferi* and other PGH from *Staphylococcus simulans* resulted in a more effective enzymes with broader specificities and higher activities[18].

Several PGHs have been identified and characterized for their potential use in food safety applications[19]. Notable examples, that include Ply500, PlyPSA, Ply 40, Ply100, Ply511, and LysZ5, have demonstrated effectiveness in controlling *L. monocytogenes* across various food matrices, providing a targeted approach to food safety[12,19–21]. The engineering of Ply500 by addition of extra copy of its CBD domain resulted in much higher activity in high salt concentration[22]. Still, the search for effective biological control of *L. monocytogenes* in food industry remians a high priority.

In this study, we present the characterization of a novel M23 peptidase from *Streptococcus thermophilus* NCTC10353 with a potent antibacterial activity. We have successfully solved its structure and demonstrated its strong efficacy against *L. monocytogenes* and *Bacillus* species, strains with *meso*-DAP-type peptidoglycan. The fusion of a cell wall targeting domain to the C-terminus significantly improved protein bacteriolytic efficacy and broadened its specificity. The chimeric enzyme StM23_CWT was further evaluated for its effectiveness against *L. monocytogenes* strains isolated from food products or food production environment. It demonstrated strong tolerance to varying pH and salt conditions compared to the EAD domain alone, retaining high activity in planktonic cultures and showing reasonable efficacy on biofilms produced by industrial strains. Additionally, it proved effective in surface decontamination tests on glass, steel, and silicone, efficiently targeting and degrading *L. monocytogenes* cell walls. Direct hydrolysis of cell wall was demonstrated by electron microscopy studies. Furthermore, thorough safety assessments conducted across various biological models, including zebrafish, moth larvae, and human cell culture systems, have conclusively demonstrated the enzyme's non-toxic properties. Overall, these findings demonstrate the strong potential of StM23_CWT as a novel and effective candidate for enhancing food safety and sanitation. Its ability to combat persistent pathogens such as *L. monocytogenes* highlights its value in reducing public health risks associated with foodborne illnesses, while ensuring a high level of safety.

Results

StM23 from *Streptococcus thermophilus* belongs to M23/M37 family of peptidases

A BLAST search with the sequence of LytM catalytic domain from *S. aureus* NCTC 83250-4 (residues 185–316, accession number : O33599) resulted in identification of putative peptidase M23/M37 in *S. thermophilus* NCTC10353 (VDG62699.1, now the record has been removed at the submitter's request). InterProScan (EMBL-EBI[23]), showed that this 225-aa long protein comprised a signal peptide (residues 1–22) and M23 peptidase domain (residues 118–214) connected via a long undefined region (residues 23–117) (Fig. 1A). The sequence alignment revealed only 31% amino acid identity to the best characterized members of M23 peptidase family, lysostaphin (lss) and LytM (Fig. 1B). However, its amino acids sequence comprises motifs characteristic for M23 peptidase family of proteins: Hx_nD and HxH that are involved in zinc binding and catalysis. The results of bioinformatic analysis was further confirmed by crystallization and structure determination of the newly identified M23 domain from *S. thermophilus*. The high-resolution X-ray data (1.35 Å) enabled the structure determination by molecular replacement, with LytM catalytic domain as the search model. The structure was refined to final R_{work} and R_{free} factors of 12.2% and 14.4%, respectively (Supplementary Table 3) and deposited in the Protein Data Bank under accession no. 9GY1.The overall fold of StM23 resembles that of other members of M23 peptidase family like lysostaphin (PDB ID: 4QPB) and LytM (PDB ID: 4ZYB) with RMSD (root-mean-square deviation) 0.96Å over 113 Cα of lysostaphin and 1.38Å over 115 Cα of LytM[24,25]. StM23 is a globular

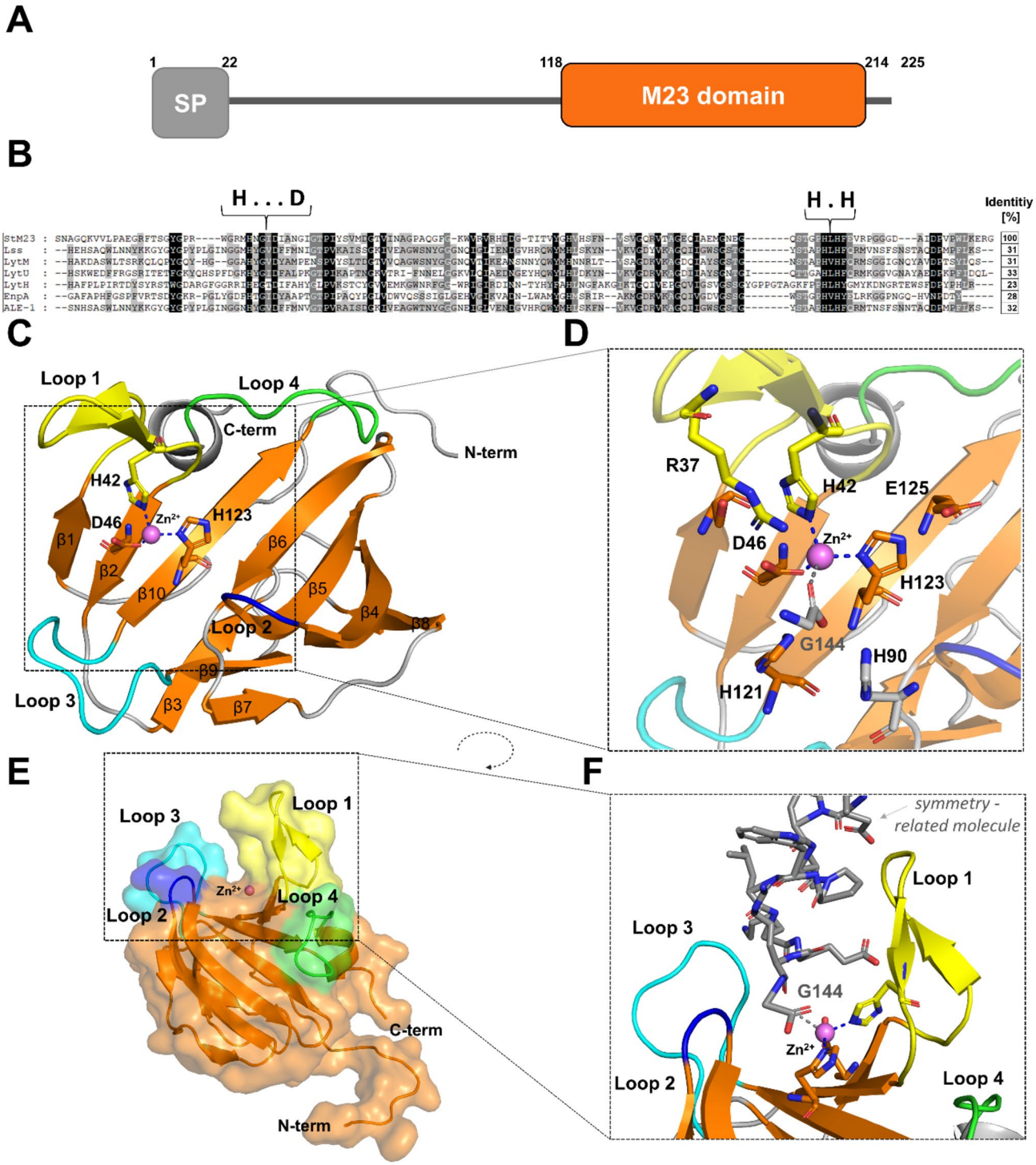

Fig. 1. Bioinformatic and structural analysis of StM23 protein (PDB ID:9GY1). (A) Domain composition of the native M23/37 peptidase identified in *S. thermophilus* NCTC 10353, highlighting key structural features. (B) Sequence conservation analysis of M23 peptidases, showing the sequence identity of StM23 compared to other related peptidases. Zinc-binding motifs **H**xxx**D** and Hx**H** are marked. (C) The overall fold of the M23 peptidase with characteristic structure of two beta sheets (orange) and distinctive loops: loop 1 (yellow), loop 2 (blue), loop 3 (cyan), and loop 4 (green), with residues involved in zinc binding highlighted. Zinc ion is shown as a purple sphere. (D) A closer view of the active site architecture, emphasizing residues that play a crucial role in catalytic function and active site stabilization. (E) Surface representation of the StM23 peptidase structure, illustrating the characteristic groove and the zinc ion (Zn^{2+}) position in the groove. (F) Close-up view of the groove with zinc ion coordination, highlighting the role of Gly144 (depicted in grey) in zinc coordination.

protein composed of two β-sheets. The central β- sheet is formed by 7 strands (β1, β2, β10, β6, β5, β4 and β8) and faces a smaller 3-stranded β- sheet (β3, β9 and β7). The loops are assigned analogously to other structures of M23 peptidases: the longest loop1 (Ser32-Ile 45) connects strands β1 and β2, the shortest loop2 (Ala69-Phe72) connects β4 with β5, loop 3 (Met111-Pro120) is located between β9 and β10, and finally loop 4 (Pro128-Asp135) connects strand β10 and a short helix in the C-terminus of the peptidase (Fig. 1C). The strong electron density of zinc ion is observed in vicinity of catalytic residues and is located in the groove formed by central β- sheet and protruding loops 1, 2 and 3 (Fig. 1C, D). The active site residues include His42 and Asp46 from the **H**xxx**D** motif, and His123 from the Hx**H** motif, all of which participate directly in Zn^{2+} coordination. The first histidine of the **H**xH motif (His121) does not serve as a zinc ligand, but it was proposed to coordinate and activate an incoming water molecule, initiating a nucleophilic attack on the scissile bond[24]. Additionally, a histidine (His90) residue located within a conserved sequence approximately 30 amino acids before the HxH motif is positioned near the active site and may also contribute to water activation. The active site architecture is stabilized by residues Arg37, Ser32 and Asp125 (Fig. 1C, D, E). Interestingly, in this crystal structure, a nucleophilic water is displaced by Gly144 from a symmetry-related molecule and its oxygen atom directly coordinates the zinc ion (Fig. 1D, F).

StM23 showed bacteriolytic activity against Gram-positive bacteria with *meso*-DAP type peptidoglycan

In the initial screening, the specificity and activity of the isolated protein were evaluated using a selection of bacterial strains characterized by distinct cell wall architectures and peptidoglycan compositions (Table 1). A significant reduction of OD was observed for *L. monocytogenes* DSM 19094 (ca. 70%) and *Bacillus subtilis* DSM 10 (ca. 65%) and moderate reduction for *Bacillus cereus* NMBU 206 (ca. 35%), all Gram-positive species with *meso*-DAP-type peptidoglycan. Interestingly, StM23 also showed some bacteriolytic activity against *Escherichia coli* DSM 10, a Gram-negative bacterium with direct *meso*-DAP-D-Ala cross-bridge. Additionally, StM23 exhibited some activity against *Lactococcus lactis* CCM 1877, resulting in a slight OD reduction of ca. 15% (Table 1; Fig. 2B).

SH3 binding domain from *S. pettenkoferi* expands tolerance to ionic strength and peptidase specificity

The specificity and activity of the chimeric protein were evaluated in a low-conductivity buffer using turbidity reduction assays on the same bacterial strains (Fig. 2, upper panel). Compared to the catalytic domain alone, StM23_CWT displayed improved efficacy against *L. monocytogenes* DSM 19094 and *B. subtilis* DSM 10, with particularly strong activity increased against *B. cereus* NMBU 206, *E. coli* DSM 1103, and *L. lactis* CCM 1877.

Bacterial strain	Type of cell wall	Type of cross-bridge in peptidoglycan (PG)	Specificity/ Activity
Escherichia coli DSM 1103	Gram (-)	*meso-DAP-D-Ala*	+
Klebsiella pneumoniae DSM 789	Gram (-)	*meso-DAP-D-Ala*	-
Pseudomonas aeruginosa DSM 939	Gram (-)	*meso-DAP-D-Ala*	-
Yersinia ruckeri CCM 4620	Gram (-)	*meso-DAP-D-Ala*	-
Bacillus subtilis DSM 10	Gram (+)	*meso-DAP-D-Ala*	+++
Bacillus cereus NMBU 206	Gram (+)	*meso-DAP-D-Ala*	++
Listeria monocytogenes DSM 19094	Gram (+)	*meso-DAP-D-Ala*	+++
Lactococcus lactis CCM 1877	Gram (+)	*L-Lys-D-Asp*	+
Enterococcus faecium DSM 2146	Gram (+)	*L-Lys-D-Asp*	-
Staphylococcus aureus NCTC 8325-4	Gram (+)	*L-Lys- Gly(5)*	-
Staphylococcus epidermidis ATCC 12228	Gram (+)	*L-Lys-Gly2-4-L-Ser1-2-Gly*	-
Staphylococcus simulans CCM 3583	Gram (+)	*L-Lys-Gly2-4-L-Ser1-2-Gly*	-
Micrococcus luteus ATCC 10240	Gram (+)	*L-Lys peptide subunit*	-
Enterococcus faecalis DSM 20376	Gram (+)	*L-Lys-L-Ala2*	-
Streptococcus agalactiae DSM 6784	Gram (+)	*L-Lys-L-Ala2*	-
Streptococcus dysgalactiae DSM 20662	Gram (+)	*L-Lys-L-Ala2*	-
Streptococcus pyogenes CCM 7418	Gram (+)	*L-Lys-L-Ala2*	-
Streptococcus uberis DSM 20569	Gram (+)	*L-Lys-L-Ala2*	-
Streptococcus canis DSM 20715	Gram (+)	*L-Lys-L-Ala2*	-
Streptococcus equi DSM 20727	Gram (+)	*L-Lys-L-Ala2*	-

Table 1. Specificity and activity of StM23 peptidase against selected Gram-positive and Gram-negative bacteria with various types of peptidoglycan cross-bridge composition as indicated. The activity was evaluated using the turbidity reduction assay at a concentration of 1 µM StM23 in 50 mM Glycine pH 8.0, incubated with bacterial suspensions (10^8 CFU/ml) for 1 h at room temperature. The degree of turbidity reduction (OD_{595}) is indicated as follows: +++ > 60% reduction, ++ 30–60% reduction, + 15–30% reduction, - < 15% no lytic activity under the tested conditions. Statistical analysis was conducted using a two-way ANOVA followed by Dunnett's multiple comparisons test. The significance levels are represented as follows: grey for $p < 0.01$, light green for $p < 0.001$, and green for $p < 0.0001$.

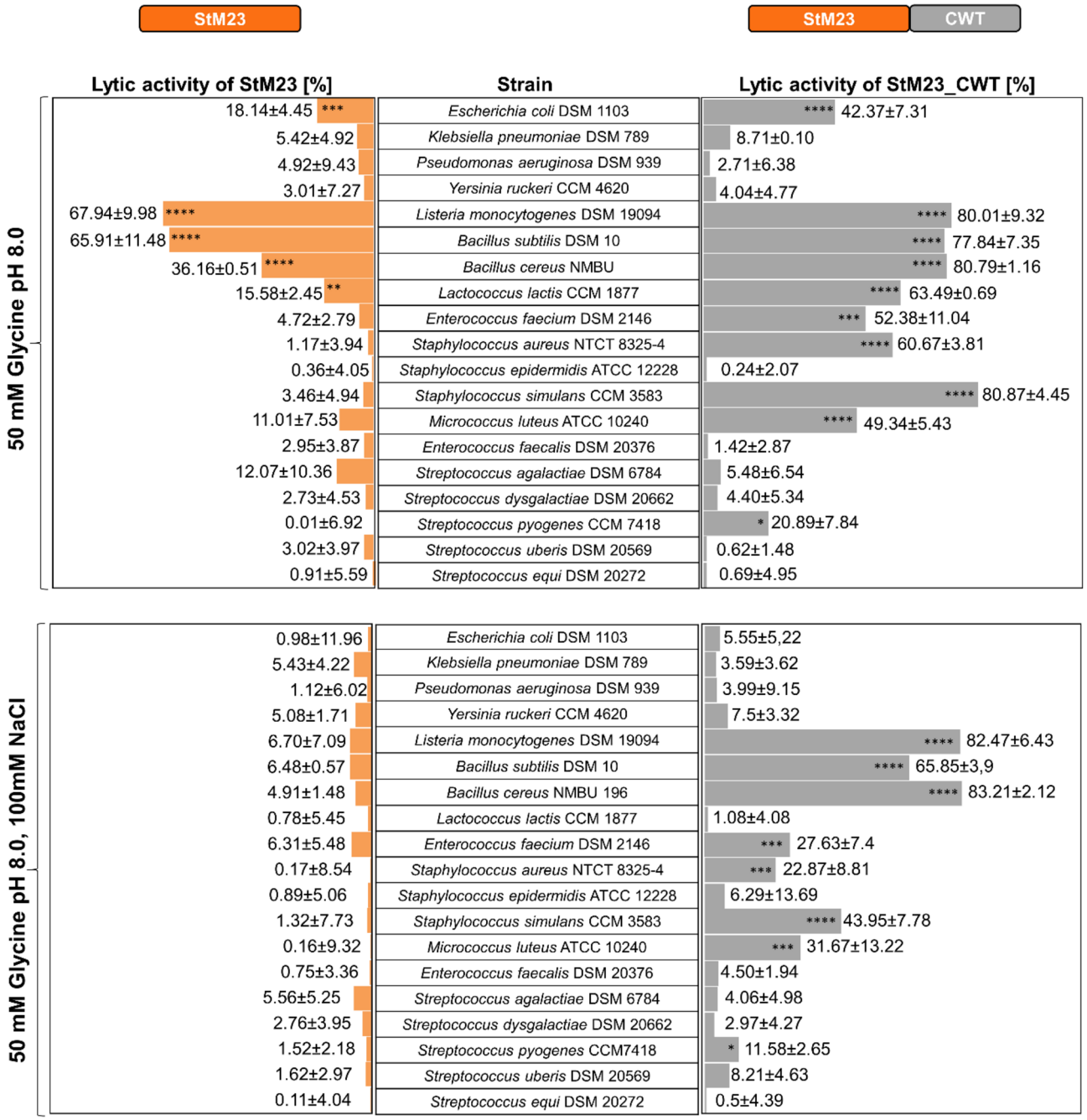

Fig. 2. Comparison of enzymatic lytic activity of StM23 and StM23_CWT enzymes on selected strains with different cell wall types as detailed in Table 1 in 50 mM Glycine pH 8.0 (upper panel) and in 50 mM Glycine pH 8.0 with 100 mM NaCl (lower panel). Lytic activity is expressed as reduction of initial OD_{595} (%) after 1 h of incubation with 1 µM enzyme. Values are adjusted by subtracting those from negative controls (bacterial suspensions incubated without added enzyme). Data are presented as mean ± SD of three replicates. Statistical analysis was performed using a two-way ANOVA with post hoc Dunnett's multiple comparisons test performed in GraphPad Prism software (version 10.0.3). Significance levels are indicated as follows: $^{*}p < 0.05$, $^{**}p < 0.01$, $^{***}p < 0.001$, $^{****}p < 0.0001$.

Unexpectedly, the enzyme's specificity expanded even further, achieving substantial OD reduction for *S. simulans* CCM 3583, *E. faecium* DSM 2146, S. aureus NCTC 8325-4 and *M. luteus* ATCC 10240 in 50 mM glycine at pH 8.0. In line with earlier observations for the LytM and lysostaphin catalytic domains[17], the presence of 100 mM NaCl was found to inhibit StM23's lytic activity (Fig. 2, lower left panel). The addition of SH3b domain from SpM23B PGH from *S. pettenkoferi* proved effective in overcoming this limitations. This particular domain was chosen due to its ability, unlike the SH3 domain from lysostaphin, to bind *L. monocytogenes* cell walls[26,27]. At 100 mM NaCl, the engineered enzyme maintained high activity against *L. monocytogenes* DSM 19094, *B. subtilis*

DSM 10, and *B. cereus* NMBU 206. Interestingly, its specificity expanded to include also *S. simulans* CCM 3583, *Enterococcus faecium* DSM 2146, *Micrococcus luteus* ATCC 10240, and *S. aureus* NCTC 8325-4 (Fig. 2, lower right panel).

Chimeric protein exhibits significantly greater tolerance to pH and salt concentrations compared to catalytic StM23

The bacteriolytic activity of the chimeric protein was analysed in comparison to StM23 lacking CWT under different pH and ionic strength conditions. A turbidity reduction assay was conducted with 1 µM enzymes incubated with *L. monocytogenes* DSM 19094 cells (OD = 1; approximately 10^8 CFU/ml). To assess the effect of pH, low ionic strength buffers of varying pH values (ranging from 5.0 to 11.0) were used. As shown in Fig. 3A, neither peptidase exhibited activity at pH 5.0. The StM23 catalytic domain showed activity only within a narrow pH range of 6.0 to 8.0, with maximum activity observed at pH 8.0. At pH 9.0, the activity of StM23 was completely abolished. In contrast, the chimera demonstrated tolerance to a much broader pH range, exhibiting high activity from pH 6.0 (approximately 70% activity) to pH 11.0 (approximately 85% activity) (Fig. 3A). Additionally, the chimera displayed significantly higher tolerance to ionic strength (Fig. 3B). While the activity of the catalytic domain was entirely inhibited by the presence of 50 mM NaCl, the chimeric protein maintained maximum activity up to a concentration of 100 mM NaCl. At 250 mM NaCl, the lytic activity decreased (with OD595 reduced by 30%). Residual activity of the StM23_CWT chimera was still observed at 500 mM NaCl, 1 M NaCl completely blocked its activity.

Furthermore, the chimeric protein acted more rapidly than the catalytic domain, reaching maximum activity within 10 min of incubation with the bacterial suspension. A 2-minute incubation period was sufficient to reduce OD by approximately 75% (Supplementary Fig. 1). The bacterial cells were then subjected to varying enzyme concentrations, with the chimera showing effective lytic activity against *L. monocytogenes* DSM 19094 after 10 min, starting at a concentration of 100 nM and resulting in an OD reduction of around 40%. The antibacterial activity increased with higher concentrations, but lytic activity plateaued once the StM23_CWT concentration exceeded 500 nM. A concentration of 1 µM was sufficient to maximally reduce turbidity within 10 min (Supplementary Fig. 2).

StM23_CWT shows bacteriolytic activity against *L. monocytogenes* under relevant food processing environment conditions

After conducting specificity and activity screening of StM23_CWT, we proceeded to test its effectiveness against *L .monocytogenes* strains isolated directly from food production facilities (MF7703, MF6331, MF5639, MF5369, MF4997, MF4991; Supplementary Table 1). These strains were provided by the Nofima research institute, ensuring that our findings are directly relevant to real-world contamination scenarios. First, a turbidity reduction assay was performed to compare the susceptibility of industrial strains to StM23_CWT. Robust bacteriolytic activity was observed against all tested strains at a concentration of 1 µM, demonstrating efficacy similar to that of the reference strain DSM 19094 (Fig. 4A).The enzyme's performance on biofilms formed by *L. monocytogenes* MF7703 on stainless steel coupons over a 24-hour period at 12 °C was also assessed, with nisin used for comparison. The MF7703 strain, known for its strong biofilm formation, reached approximately 10^7 CFU/coupon. Treatment with 1 µM StM23_CWT led to a ~ 0.8 log reduction in biofilm cell count (ca. 84.15% of bacteria were killed), comparable to the reduction observed with nisin. No synergistic effect was detected when both compounds were used together. However, increasing the enzyme concentration to 5 µM resulted in a more

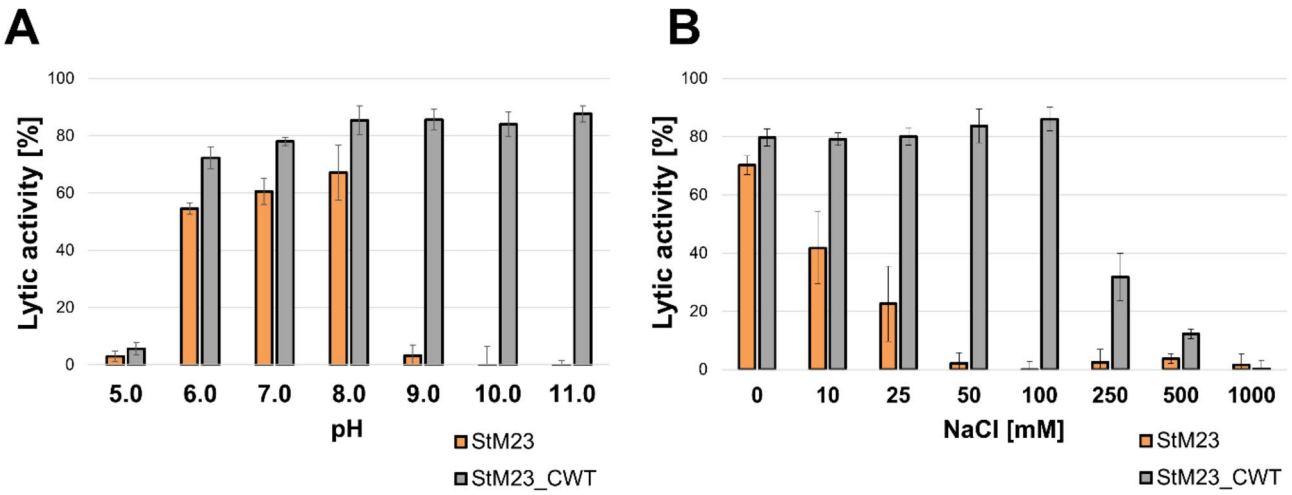

Fig. 3. Comparison of enzyme activity at varying pH levels and salt concentrations for StM23 (orange) and StM23_CWT (grey) on *L. monocytogenes* DSM 19094. (A) pH dependence of StM23 and StM23_CWT in low conductivity buffers at different pH levels (ranging from 5 to 11); (B) Salt concentration dependence of StM23 and StM23_CWT activity in 50 mM glycine buffer at pH 8.0 with increasing NaCl concentrations (from 0 to 1000 mM). Data are presented as mean ± SD of three replicates (3 wells per replicate).

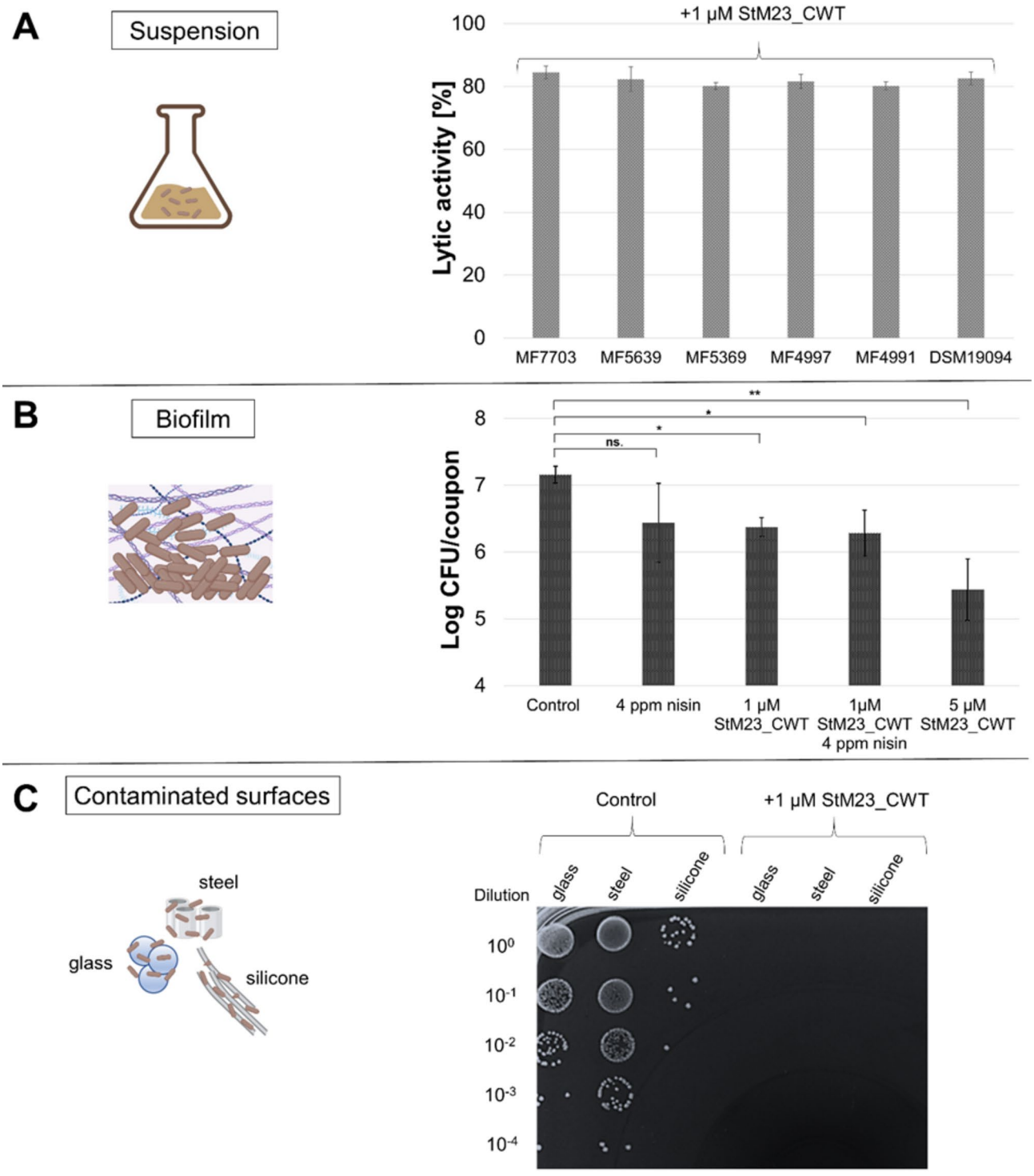

Fig. 4. Bacteriolytic effects of the StM23_CWT chimera in food production environment relevant conditions. (A) Lytic activity [%] of the enzyme on *L. monocytogenes* strains isolated from food processing environment by Nofima, compared to the DSMZ strain. (B) Bactericidal effect (LOG CFU/coupon reduction) of the chimera on *L. monocytogenes* MF7703 biofilm at 1 µM and 5 µM concentrations treated for 24 h at 12 °C. Nisin at 4 ppm was used as a control and for synergy studies. Data are presented as mean ± SD of three replicates. Statistical analysis was performed using one-way ANOVA with post hoc Tukey test. Significance levels are indicated as follows: $*p < 0.05$, $**p < 0.01$. (C) Results of enzymatic surface decontamination of *L. monocytogenes* MF7703 on glass, stainless steel, and silicone surfaces treated with 1 µM enzyme for 1 h at room temperature.

substantial reduction of approximately 1.7 log (ca. 98% of killed bacteria), indicating improved efficacy at higher concentrations (Fig. 4B).

Following these findings, the bactericidal effect of StM23_CWT was tested in a surface decontamination assay. Glass beads, stainless steel cylinders, and silicone tubes were inoculated with *L. monocytogenes* MF7703 (10^8 CFU/ml), air-dried, and treated with either a buffer (control) or buffer containing 1 µM StM23_CWT enzyme for 1 h at room temperature. Serial dilutions and spot assays were performed to visualize remaining viable bacteria, allowing for the assessment of bacterial attachment and enzymatic decontamination effectiveness. The results showed strong adhesion of *L. monocytogenes* to the stainless steel cylinders (observed 10^7 CFU/ml which corresponds to 7×10^5 CFU/cm^2) and to glass beads (10^6 CFU/ml which corresponds to 1.7×10^5 CFU/cm^2) whereas significantly weaker attachment was observed on silicone tubes, with levels ranging between 10^3 and 10^4 CFU/ml (corresponding to only 0.5×10^3 CFU/cm^2). Bacteriolytic treatment with StM23_CWT successfully eradicated all bacterial contamination on all tested surfaces, with no detectable bacterial growth following treatment (Fig. 4C). These findings suggest that StM23_CWT is highly effective in eliminating planktonic *L. monocytogenes* as well as attached to various surfaces, including those commonly used in the food industry, such as stainless steel.

StM23_CWT led to bacterial cell damage confirmed by electron microscopy studies

The impact of StM23_CWT on the ultrastructure of *L. monocytogenes* MF7703 was investigated using both transmission electron microscopy (TEM) and scanning electron microscopy (SEM) (Fig. 5). The minimum inhibitory concentration (MIC) of StM23_CWT for *L. monocytogenes* MF7703 was determined to be 62.5 nM. For the microscopy studies, optimal concentrations were set at 1xMIC and 2xMIC values. TEM analysis of untreated *L. monocytogenes* cells revealed well-preserved structures with intact cytoplasmic membranes, cell walls, and dense cytoplasmic content (Fig. 5A-C). Following exposure to StM23_CWT, bacterial cell wall damage was evident, resulting in severe lysis at both 1xMIC and 2xMIC along with the accumulation of cell debris (Fig. 5E, I). These images clearly demonstrated cell wall disruption and leakage of cytoplasmic contents caused by enzyme treatment (Fig. 5F, J, G, K). SEM analysis confirmed these observations (Fig. 5D, H, L). Notable reduction in intact *L. monocytogenes* cells was observed especially at the 2xMIC concentration (Fig. 5L). The remaining cells displayed severe structural damage, including shrinkage, with wrinkled and ruptured membranes, indicating extensive lysis caused by StM23_CWT (Fig. 5L).

The safety of StM23_CWT confirmed in various biological models

Developmental toxicity has been evaluated in the zebrafish model using modified OECD test no 236. The mortality rates, malformation rate, and morphological abnormalities were recorded daily. The embryos which were exposed to 1 µM StM23_CWT from 4 to 96 hpf developed normally, had similar body length and overall morphology as untreated control zebrafish larvae (Fig. 6A). The survival rate also was unaffected and all fish survived till 96hpf, when experiment ended (data not shown). Toxicity of StM23_CWT also was assessed in *Galleria mellonella* larvae, a model that allows for the rapid assessment of compound toxicity *in vivo.* The development and mortality of *G. mellonella* larvae injected with 1 µM StM23_CMT, mock-injected control and untreated larvae were monitored for seven days. In all groups, the survival rate was high (Fig. 6B) and the survival curves did not differ statistically when analysed controls and treated group in GraphPad Prism. *G. mellonella* larvae developed normally, progressing through expected stages, including cocoon formation and pupation. Malanization, a visual indicator of stress, also was not triggered upon the treatment (data not shown). Hence, StM23_CWT can be classified as non-toxic to *G. mellonella* larvae. Moreover, the cytotoxicity of StM23_CWT was evaluated in vitro using the MTT assay. After 24 h of exposure to 1 µM and 5 µM StM23_CWT, the metabolic activity of mouse fibroblasts (NIH 3T3) and human keratinocytes (HaCAT) remained comparable to that of the untreated control (Fig. 6C). However, it should be pointed out that cell metabolic activity was slightly reduced after 5 µM StM23_CWT-treatment.

Discussion

Food contamination is a significant public health concern that can lead to foodborne illnesses, with substantial economic and social costs[28]. Bacterial contamination is a leading cause of hygiene issues and elevated spoilage rates, contributing substantially to food waste and loss[29]. In food production systems, bacteria are mainly found attached to surfaces or embedded in biofilms. These surface-associated or biofilm-embedded bacteria display much greater resistance to environmental stresses, including sanitation methods, than their free-floating (planktonic) counterparts[30,31]. Addressing *L. monocytogenes* contamination is especially challenging for food processors due to its ubiquitous nature, ability to proliferate at refrigeration temperatures, and its propensity to form biofilms that result in persistent contamination and severe health risks. Consequently, there is an urgent need for innovative control strategies to ensure the sustainable production of safe, high-quality foods.

This study contributes to these efforts by identifying and characterizing a new bacteriolytic enzyme, which holds significant promise for enhancing food safety, particularly *against L. monocytogenes*. The investigation commenced with the identification of an M23 peptidase from *S. thermophilus* NCTC10353, followed by its cloning, overexpression, purification, and structural characterization. The enzyme belongs to the M23 family of zinc metallopeptidases, recognized for their ability to efficiently hydrolyze peptidoglycan in both Gram-positive and Gram-negative bacteria[32]. Certain M23 peptidases are particularly promising for bacterial control due to their high efficiency, specificity, and ease of modification, which enables performance optimization[18,19,33,34]. One prominent application of modified M23 enzymes is the commercially available Staphefekt SA.100, a dermocosmetic agent targeting *S. aureus*. This bacteriolytic enzyme originating from the 2638A endolysin from staphylococcal phage, was modified by substituting its M23 domain with that of lysostaphin, significantly improving its efficacy against *S. aureus*, including methicillin-resistant strains (MRSA)[35].

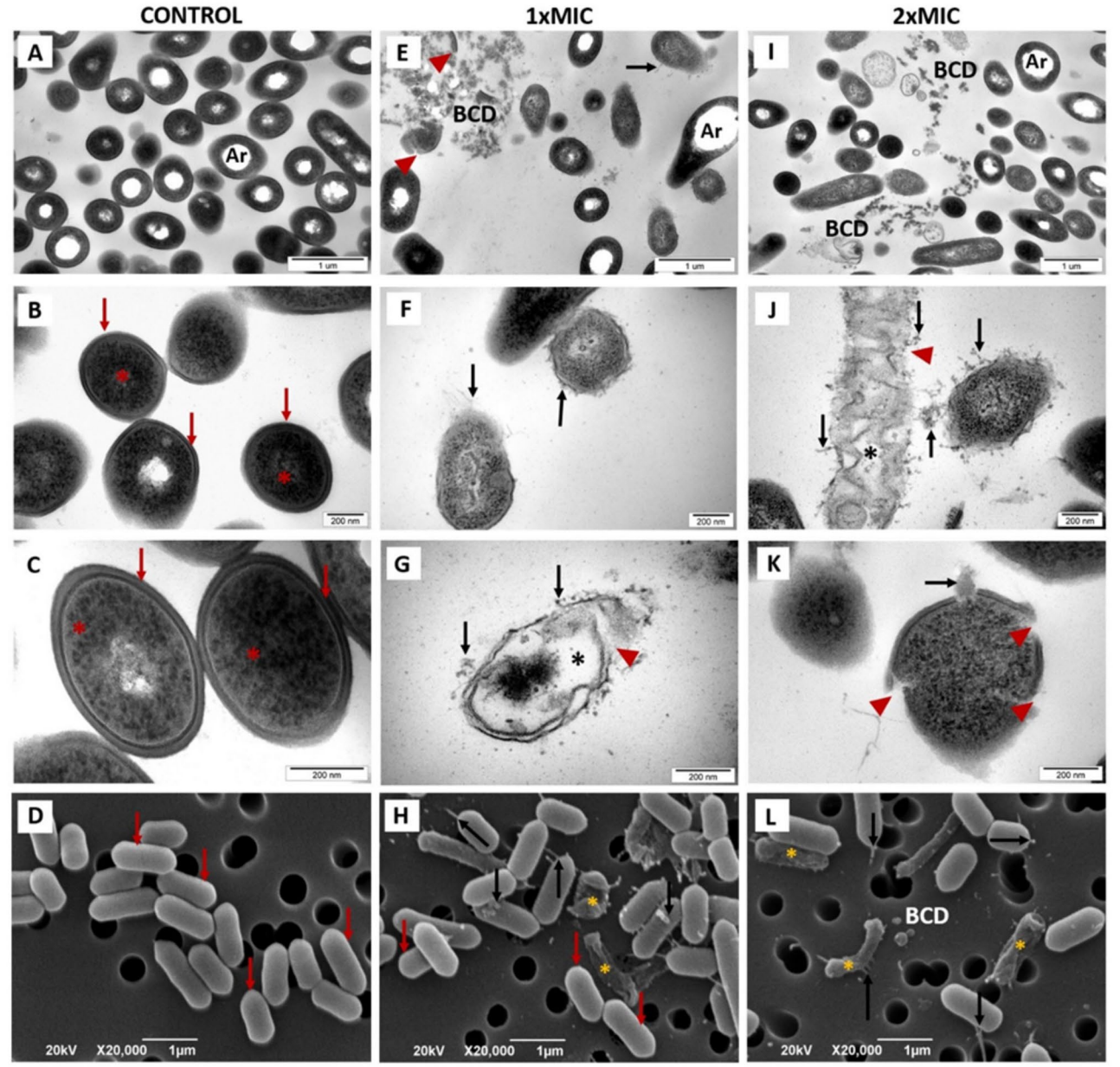

Fig. 5. Lytic activity of the StM23_CWT protein on *L. monocytogenes* MF7703, as demonstrated by transmission (TEM, upper rows) and scanning (SEM, bottom row) electron microscopy studies. In the control group, no ultrastructural changes were observed, with electron micrographs showing intact, complete bacterial cell walls (A-D, red arrows) and electron-dense cytoplasmic content (B, C, red stars). In contrast, cells treated with StM23_CWT (E-L) exhibited a wide range of ultrastructural alterations. At both 1xMIC (E-H) and 2xMIC (I-L), significant bacterial cell damage was noted, including cell wall disruption (E, G, J, K, red arrowheads), leakage of cytoplasm (E- L, black arrows), accumulation of bacterial cell debris - BCD (E, I), loss of cytoplasm resulting in presence of cytoplasmic clear zones (G, J, black stars). In SEM analysis, at 1xMIC (H) group, only a few well-preserved cells were noted (red arrows), while the majority exhibited severe structural damage, including shrinkage (yellow stars) and cytoplasmic leakage (black arrows). At 2xMIC concentration (L), all cells displayed ultrastructural alterations (shrinkage and cytoplasmic leakage) and bacterial cell debris accumulation (L). Some artifacts- Ar (A, E, I), caused by sectioning procedure were comparable in all groups.

In this study, the M23 peptidase from *S. thermophilus* (StM23) was evaluated for its potential application in controlling *L. monocytogenes*. However, isolated M23 domains typically exhibit reduced bacteriolytic activity in high ionic strength environments, limiting their independent efficacy. To address this limitation, based on previous results for LytM and EnpA[17,18], a chimeric peptidoglycan hydrolase was constructed by fusing the SH3b domain of the SpM23B peptidoglycan hydrolase from *S. pettenkoferi* to the C-terminus of StM23. This specific SH3b domain has demonstrated effective binding to both Gram-positive and Gram-negative bacteria, irrespective

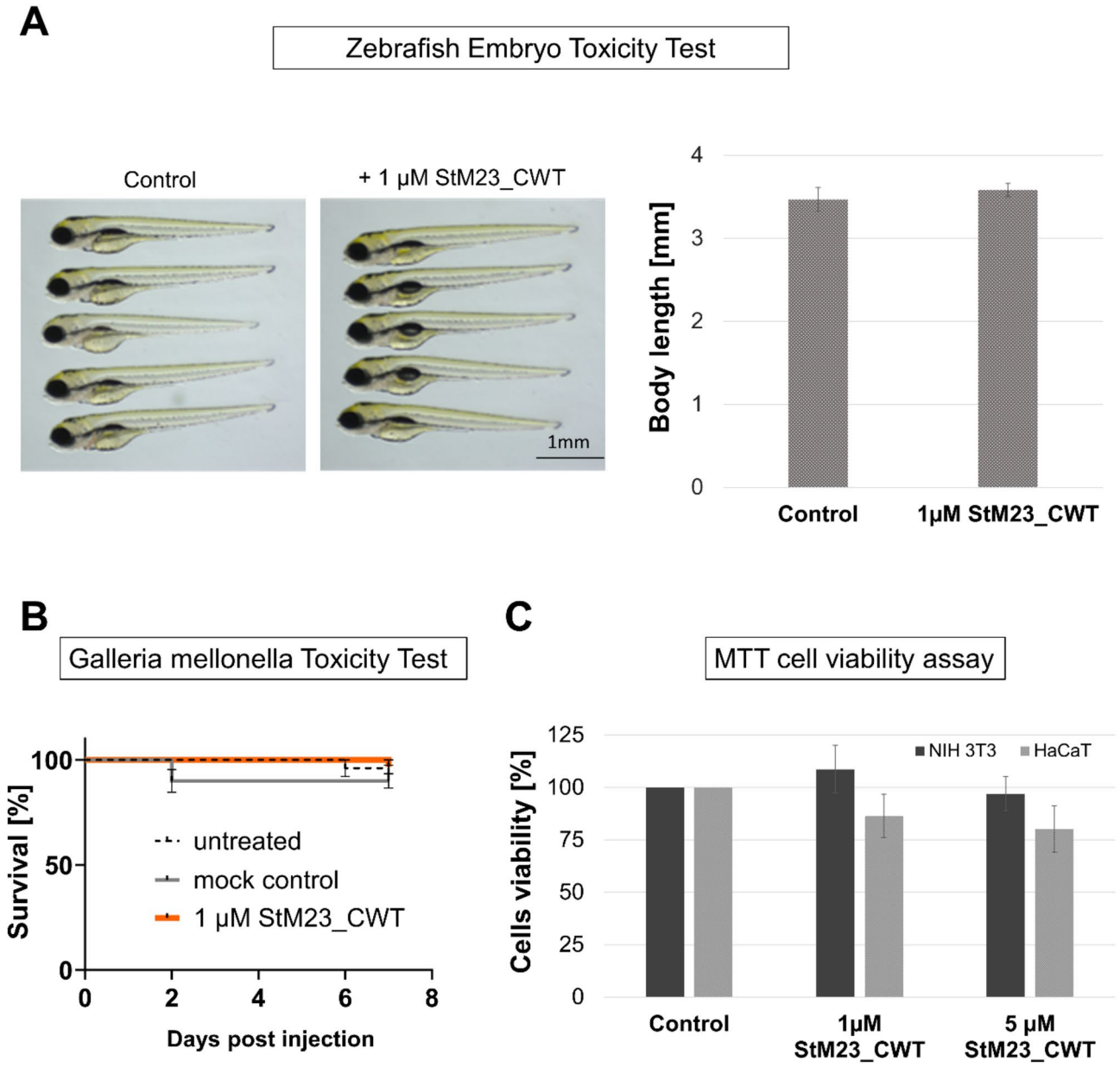

Fig. 6. Safety profile of StM23_CWT. (A) Unchanged morphology of zebrafish larvae at 96 hpf. Left panel shows lateral views of control and zebrafish larvae treated with 1µM StM23_CWT. Bar plot (right panel) demonstrate unchanged body length of zebrafish one of the indicators of unaffected development. Scale bar = 1 mm. (B) The Kaplan-Meier plots show the percentage of *G. mellonella* larvae surviving challenge with StM23_CWT. (C) The results of the MTT assay on mouse fibroblasts (NIH 3T3) and human keratinocytes (HaCAT) for 1 µM and 5 µM are presented as the percentage of cell viability. Error bar shows SD ($n = 3$ replicates, 9 wells per replicate).

of variations in their peptidoglycan structure[27]. The chimeric protein StM23_CWT exhibited improved efficiency across a broad pH and salt range, effectively targeting other significant foodborne contaminants such as *S. aureus*. It has to be mentioned, that chimera also demonstrated activity against *L. lactis*, a beneficial bacterium widely used in food production. However, this activity could be selectively diminished under high-ionic-strength conditions (e.g., 100 mM NaCl), enabling the targeted inhibition of pathogens while preserving beneficial bacteria. The activity of StM23_CWT is exceptionally high (> 80%) on planktonic cells compared to other endolysins, such as PlyPSA and Ply40, which exhibit a maximum lytic activity of approximately 40% in the turbidity reduction assay[21]. However, *L. monocytogenes* contamination often originates from surfaces or equipment in processing environments, where biofilms pose persistent contamination risks. This bacterium readily adheres to common food-processing surfaces like stainless steel, silicone, and glass, with biofilm formation influenced by factors like strain, temperature, pH and nutrient availability[36]. The growing prevalence of antimicrobial resistance (AMR) intensifies the need for innovative strategies in pathogen control and food preservation. Bacteriophage-based

solutions, such as PhageGuard Listex™ P100, approved by the FDA and EU, have proven effective in reducing *L. monocytogenes* in ready-to-eat foods, including meat, poultry, fish, and dairy products[37]. Similarly, lactic acid bacteria (LAB) enhance food safety by producing antimicrobial compounds, such as bacteriocins and organic acids, which have proven effective in reducing *L. monocytogenes* under refrigeration[38,39]. One of the most well-known and widely studied bacteriocins is nisin, which has been also approved by both the FDA and EU for use as a food preservative[40]. Nisin is a naturally occurring antimicrobial peptide produced by *Lactococcus lactis*, that belongs to a class of antibacterial compounds known as lantibiotics, highly effective against Gram-positive bacteria, including *Listeria*, *Staphylococcus*, *Clostridium*, and *Bacillus*, primarily by forming pores in the bacterial membrane[40,41]. Due to its potent antimicrobial properties, nisin has been widely employed in the food industry to control *L. monocytogenes* in products such as dairy, meat, and canned products[42,43]. However, nisin is most effective in acidic environments, which aligns with the pH of many food products such as dairy and fermented foods[44]. Nisin's activity decreases in neutral or alkaline environments, where it tends to become less stable and more susceptible to degradation. This pH sensitivity can limit its effectiveness in certain food systems, making the use of complementary antimicrobials effective in alkaline conditions, such as our chimeric protein, highly advantageous. StM23_CWT exhibits strong activity in the pH range between 6 and 11, making it particularly useful in more physiological conditions. Moreover, an increasing number of bacterial strains are developing resistance to nisin, further highlighting the need for complementary approaches[45]. *L. monocytogenes* poses a significant challenge due to the increased resistance of biofilm-grown cells to conventional disinfectants. While *L. monocytogenes* in suspension is generally susceptible to most disinfectants, the bacteria become less susceptible when they adhere to surfaces. This resistance varies with biofilm age and thickness, as cells in old or thicker biofilms show greater resistance to common disinfectants like benzalkonium chloride, sodium hypochlorite and peracetic acid[31,46]. Additionally, *L. monocytogenes* may show enhanced survival in multispecies biofilms exposed to biocides by means of interspecies interactions and protection compared to biofilms composed solely of *L. monocytogenes*[31,47]. While endolysins have been extensively studied for their role in preventing biofilm formation, their effectiveness in removing well-established biofilms remains underexplored[48,49]. For instance, the PlyLM amidase achieved only a modest reduction of biofilm by approximately 20% when applied alone. Significant removal of the biofilm was observed only when PlyLM was combined with proteinase K treatment, which suggests that combination treatments may be essential for effectively disrupting mature *L. monocytogenes* biofilms[50]. These findings emphasize the importance of further research to improve endolysin effectiveness against bacteria on surfaces and within biofilms, which present major challenges for food safety and hygiene management. Our research expanded on this issue by focusing on biofilms cultivated for 48 h at 12 °C, a setting that resembles real-world environments typical of food processing. When the chimeric StM23_CWT enzyme was tested on these mature biofilms, it achieved substantial reduction in the bacteria embedded within the biofilm. However, since this experiment was conducted at 12 °C, a temperature that may limit hydrolase activity, the results suggest that the enzyme could be even more effective under optimized conditions. Importantly, the engineered StM23_CWT enzyme showed high effectiveness in decontaminating materials commonly used in food production and it proved to be safe. Future research will focus on testing StM23_CWT under different environmental conditions and against a broader range of bacterial targets, including *B. cereus*, *B. subtilis*, and *S. aureus*, which are commonly found in food processing settings[51–53] and on multigenus biofilms of e.g. *L. monocytogenes* and bacterial genera (e.g. *Pseudomonas* spp.) often dominating in *L. monocytogenes* high risk food production environments[54].

Chimeric enzymes with peptidoglycan hydrolase activity hold considerable promise in the food industry, particularly as natural antimicrobial agents against foodborne pathogens. However, despite their advantages, several limitations and challenges remain unresolved. Their stability can be influenced by factors such as temperature, pH, and storage conditions, which may reduce their effectiveness during food processing and storage. Additionally, PGHs often exhibit a narrow spectrum of activity, targeting specific bacterial strains, which may limit their application across a wide range of food products. The high cost of large-scale production and potential interference with complex food matrices may further restrict their use as broad-spectrum antimicrobial agents. While bacterial resistance remains a concern, preliminary results are promising. These challenges underscore the importance of continued research to improve the stability, spectrum, and cost-effectiveness of PGHs, as well as to develop strategies to mitigate the risk of bacterial resistance. Addressing these issues will be key to making PGHs a viable and widely accepted solution for food preservation and safety.

Materials and methods

Identification of StM23 from *S. thermophilus* NCTC10353 as putative peptidoglycan hydrolase

The amino acid sequence of the LytM catalytic domain (residues 185–316) was used as the query sequence for a BLAST (Basic Local Alignment Search Tool) search. This search was performed against streptococcal genomes within the non-redundant protein database available on the National Center for Biotechnology Information (NCBI) platform. BLAST parameters were set to default, and sequences with significant similarity were selected for further analysis.

Bacterial strains, plasmids and culture conditions

The bacterial strains used in this study were obtained from several sources, including the German Collection of Microorganisms and Cell Cultures GmbH (DSMZ), the American Type Culture Collection (ATCC), the Czech Collection of Microorganisms (CCM), and the Norwegian food research institute Nofima. The *B. cereus* NMBU 206 strain was generously provided by Norwegian Institute of Life Science (NMBU). A complete list of strains and their sources is placed in Supplementary Table 1. Strains were routinely cultured in Tryptic Soy Broth (TSB) at 37 °C with shaking at 80 rpm. Protein overexpression was carried out using *Escherichia coli* BL21

(DE3). Pre-cultures of *E. coli* BL21 (DE3) were grown in LB broth Lennox (Bioshop Canada Inc.), while protein overexpression was performed in Super Broth auto-induction medium (Formedium).

The gene encoding the full-length putative M23/37 peptidase from *S. thermophilus* NCTC10353 was codon-optimized and synthesized by BioCat Company (Germany). A C-terminal fragment containing the enzymatically active domain (EAD) StM23 (residues 97–222 of VDG62699.1) was subcloned into the pET His6 TEV LIC cloning vector (1B), a plasmid provided by Scott Gradia (Addgene plasmid #29653), following the protocol provided by Addgene. The chimeric protein StM23_CWT was constructed using the Polymerase Incomplete Extension (PIPE) cloning method. The CWT domain (residues 348–446 of protein ASE36562.1 from *Staphylococcus pettenkoferi*) was cloned from the vector containing other chimeric protein with the same CWT domain (EP chimera[18]). In PIPE method, the insert and vector were amplified separately using I-PIPE and V-PIPE primers, respectively, and then mixed to create vector-insert hybrids as outlined in the PIPE cloning protocol[55] (Supplementary Table 2).

Protein overexpression and purification

Escherichia coli BL21 (DE3) bacteria containing the appropriate plasmid and antibiotic (kanamycin final 50 µg/ml) were grown at 37 °C for 3 h, followed by protein expression at 25 °C for an additional 20 h. The cells were collected by centrifugation for 15 min at 5,000xg and the pellet was kept at -20 °C until use.

Purification of StM23

The cell pellet was resuspended in a buffer A (50 mM TRIS-HCl, pH 7.5; 200 mM NaCl; 20 mM imidazole; 10% (v/v) glycerol), and the cells were lysed by sonication. The lysate was centrifuged at 20,000xg for 30 min, and the resulting supernatant was loaded onto Talon beads (TALON® Superflow™, Cytiva) packed into an Econo-Column® Chromatography Column (Bio-Rad) using a peristaltic pump. After washing the beads with buffer A, the protein was eluted using buffer B (50 mM TRIS-HCl, pH 7.5; 200 mM NaCl; 500 mM imidazole; 10% (v/v) glycerol). The eluted fractions were analyzed by 15% SDS-PAGE, and those containing the desired protein were pooled, concentrated, and further purified by size-exclusion chromatography using a HiLoad Superdex 75 Increase 16/600 GL column connected to an Äkta Purifier system (Cytiva). The size-exclusion buffer consisted of 50 mM TRIS-HCl, pH 7.5; 100 mM NaCl; and 10% (v/v) glycerol.

Purification of chimeric StM23_CWT protein

Cells expressing the chimeric protein were resuspended in a buffer C (50 mM TRIS-HCl, pH 7.5; 1 M NaCl; 20 mM imidazole; 10% (v/v) glycerol), lysed by sonication, and centrifuged as described above. The supernatant was diluted with buffer D (50 mM TRIS-HCl, pH 7.5; 20 mM imidazole; 10% (v/v) glycerol) to a final salt concentration of 300 mM NaCl. The solution was then loaded onto Talon beads, and the protein was purified and then polished by size-exclusion chromatography, following the same procedure as for the catalytic domain. However, in this case, the buffer used for SEC chromatography contained 200 mM NaCl instead of 100 mM NaCl.

Peak fractions containing purified StM23 or StM23_CWT proteins were pooled, concentrated, and aliquots were flash-frozen in liquid nitrogen and stored at − 80 °C.

Protein crystallization and structure determination of StM23

StM23 protein was concentrated up to 9 mg/ml and subjected to crystallization at 18 °C by the sitting-drop vapor diffusion method using crystallization robot (Phoenix) at the IIMCB core facility and crystallization screens Morpheus (Molecular Dimensions), Natrix (Hampton Research) and JBScreen JCSG++ (Jena Bioscience). Many crystals appeared overnight on plate with Natrix crystallization buffers. The best diffracting crystals of StM23 were obtained upon incubation with an equal volume of reservoir buffer that contained 0.05 M sodium cacodylate trihydrate pH 6.5; 0.08 M magnesium acetate tetrahydrate and 30% (w/v) polyethylene glycol 4000. Crystals were cryo-protected in 30% (v/v) glycerol and flash frozen in liquid nitrogen. The X-ray diffraction data for StM23 domain crystals were collected at the PETRA III storage ring at beamline P14 (EMBL, Hamburg, Gemany). The dataset was processed and scaled using the XDS/XDSAPP GUI[56,57]. The StM23 crystals belonged to the P61 space group and contained 1 molecule per asymmetric unit. The structure was solved with PHENIX Phaser-MR[58] using LytM catalytic domain structure as a search model (PDB ID: 4ZYB). The structure was refined in phenix.refine[59] with manual building in Coot[60]. The RMSD values were calculated in Coot. The figures with StM23 structure were generated using Pymol (PyMOL Molecular Graphics System, version 2.2, Schrödinger, LLC; http://pymol.org/).

Evaluation of proteins activity and specificity using turbidity reduction assay

A total of 20 bacterial strains (Table 1) were used to test activity of enzymatically active domain StM23 and StM23_CWT chimera using turbidity reduction assay (TRA). Bacterial strains were cultured in fresh TSB medium from overnight cultures until they reached the mid-exponential growth phase (OD_{600} 0.6–0.8). After harvesting, the cells were resuspended in 50 mM Glycine pH 8.0 or 50 mM Glycine pH 8.0 with 100 mM NaCl to reach an OD_{600} of approximately 1.0, corresponding to around 1×10^8 CFU/ml. A 100 µl aliquot of protein solution (final concentrations 1 µM of StM23 (15 µg/ml) and StM23_CWT (27 µg/ml)) in the appropriate buffer was added to each well of a 96-well plate, followed by an equal volume of bacterial cell suspension. The turbidity was measured every 2 min over a 1-hour period at 595 nm using a Bio-Rad plate reader. Each experiment was conducted three times, with each sample prepared in triplicate. Lytic activity was calculated as the difference between the OD of the negative control (bacterial cells without enzyme) and the OD of cells treated with the appropriate enzyme after 1 h of incubation and presented as percentage [%] of OD reduction.

Characterization of proteins activity at different conditions

The turbidity reduction assay described above was used to identify the optimal lytic conditions for both proteins. To determine the pH optima, StM23 and StM23_CWT were tested across a pH range of 5 to 11 using low-conductivity buffers: 10 mM sodium acetate pH 5.0, 2 mM sodium citrate pH 6.0, 5 mM TRIS-HCl pH 7.0, 50 mM Glycine pH 8.0, 50 mM TRIS-HCl pH 9.0, 20 mM CAPS pH 10.0, and 10 mM CAPS pH 11.0. For determining salt optima, the proteins were tested in 50 mM Glycine pH 8.0 supplemented with increasing concentrations of NaCl, ranging from 0 to 1000 mM.

Surface decontamination test

Three different materials (glass, stainless steel and silicone) were contaminated with *L. monocytogenes* MF7703. Bacterial cells were cultured overnight in tryptic soy broth (TSB), centrifuged, and resuspended in sterile water to achieve a McFarland value of 1.8, corresponding to approximately 5×10^8 CFU/ml. Sterile glass beads (8 mm diameter), stainless steel cylinders (10 mm long, 8 mm external diameter, 6 mm internal diameter), and silicone tubes (18 mm long, 5 mm external diameter, 2 mm internal diameter) were incubated in a bacterial suspension (1×10^8 CFU/ml) and air-dried under sterile conditions for 30 min. The contaminated materials were then incubated for 60 min in 2 ml of 1 µM StM23_CWT in a buffer containing 50mM Glycine pH 8.0 and 100 mM NaCl at room temperature. A control group, which was a buffer without the enzyme, was included in the experiment. Following treatment, serial dilutions were prepared in 50 mM Glycine pH 8.0; 100mM NaCl, and the samples were plated on Tryptic Soy Agar (TSA) to assess bacterial survival via spot dilution assay.

Spot dilution assay

Cells at the desired density were subjected to 10-fold serial dilutions, and 5 µl of each dilution was plated onto TSA plates. The plates were incubated overnight at 37 °C, and results were recorded the following day. Each sample was plated in triplicate, and the experiment was independently repeated three times.

Biofilm reduction assay

The *L. monocytogenes* MF7703 was cultivated from frozen stock cultures on Tryptic Soy Agar (TSA) overnight at 37 °C. A single colony of the strains were individually cultured in TSB at 37 °C overnight and diluted 1:100 to approximately 10^7 CFU/ml in fresh TSB. 5 ml of the suspensions were pipetted into each well of a six-well tissue culture plate (Multiwell 6-well Falcon; Corning Incorporated, USA) containing a single 20 × 20 mm coupon of stainless steel (AISI 304, 2B, Norsk Stål AS, Nesbru, Norway) in each well. The culture plates were incubated at 12 °C for 48 h for biofilm formation on the coupons followed by pipetting off the culture suspensions. The coupons were rinsed in reaction buffer (50 mM Glycine pH 8.0 with 100 mM NaCl) to remove planktonic cells. Bactericidal effects to the *L. monocytogenes* biofilm were determined by the addition to each well with coupons 2 ml of appropriate concentrations of StM23_CWT (1000–5000 nM), nisin (4 ppm; Nisin from Lactococcus lactis N5764, Sigma-Aldrich) or both prepared in 50 mM Glycine pH 8.0 with 100 mM NaCl reaction buffer; controls being reaction buffer only. The biofilms were treated for 24 h at 12 °C. After treatment, the coupons were transferred to glass tubes with 5 ml peptone water. The tubes were put in a sonication water bath (60 Hz for 10 min; Bransonic 3510) to dislodge the adherent cells from the coupon. Sonicated cell suspensions were spiral plated on TSA (37 °C, 48 h) to determine CFU of enzyme-treated and non-treated (buffer only) biofilms on coupons.

MIC determination

The minimum inhibitory concentration (MIC) of StM23_CWT was determined using a broth microdilution method in 96-well plates, following a previously described protocol, with the modification of using 25% tryptic soy broth (TSB) instead of CAMBH medium. This adjustment was made as 25% TSB provided optimal bacterial growth conditions without affecting the enzyme's activity. Briefly, overnight cultures of *L. monocytogenes* DSM 19,094 were transferred into 25% TSB and incubated at 37 °C for three hours. A suspension of 5×10^5 CFU/mL was prepared, and 100 µL of it was dispensed into each well. Purified StM23_CWT enzyme was then added at concentrations ranging from 15.625 nM (0.41 µg/mL) to 8000 nM (214 µg/mL). The plate was incubated at 37 °C for 20 h, after which the MIC was determined as the lowest enzyme concentration that completely inhibited bacterial growth. The MIC for the other strains was determined using the same methodology.

Electron microscopy

Scanning (SEM) and transmission (TEM) electron microscopy was performed according to protocol described previously with some modifications[61]. Briefly, *L. monocytogenes* MF7703 strain was grown overnight in TSB medium at 37 °C with 80 rpm shaking. The cells were centrifuged and diluted in 50 mM Glycine pH 8.0, 100 mM NaCl to 4 McFarland (ca. 10^9CFU/ml). Then the cells were incubated with 1xMIC and 2xMIC dose of StM23_CWT for 60 min at RT. The control - cells without enzyme treatment were kept only in a buffer. For TEM, cell pellet was subjected to experimental procedure, whereas for SEM, the samples were loaded onto 0.4 µm-pore size membrane filters (Isopore, 13 mm diameter). The bacterial cells were fixed using 2.5% glutaraldehyde solution in 0.1 M cacodylate buffer for 2 h. Then samples were washed in 0.1 M cacodylate buffer and postfixed with osmium tetroxide 0.2% solution, followed by dehydration in an ethanol gradient. Next, for TEM analyses bacteria were embedded in epoxy resin Embed 812 (Serva, Heidelberg, Germany). The ultra-thin sections were stained with uranyl acetate for 15 min followed by lead citrate for 5 min. Images were acquired using a JEM-1011 EX transmission electron microscope (Jeol, Tokyo, Japan) equipped with a MORADA camera and Analysis image processing iTEM v.1233 software (Olympus Soft Imaging Solutions, GmbH, Münster, Germany). For SEM analyses samples after dehydration were dried using liquid CO_2 in a critical point drier B7020 (Agar Scientific)

and spray-coated with a thin gold layer in sputter coater SC7620 (POLARON). Images were acquired using a JSM-6390LV scanning electron microscope (Jeol, Tokyo, Japan).

Safety profile of StM23 evaluation

Acute toxicity – vertebrate model

Wild-type AB^{OMD}zebrafish (*Danio rerio*) breeding pairs were obtained from the Experimental Medicine Center (OMD) in Lublin, Poland, and housed at the Aquatic Facility of the Mossakowski Medical Research Institute, Polish Academy of Sciences (breeder license number 026 and used licence number 0093, issued by the Ministry of Science and Higher Education in Poland). Thirty to sixty adult fish, aged 3 to 20 months, were maintained in a 100 L glass tank filled with 75 L of water under a 14-hours light/10-hours dark photoperiod. Water parameters were maintained as follows: temperature 26 °C ± 0,5 °C, pH 7.0-7.5, conductivity 300–400 µS/cm^2, with undetectable levels of NO_2^- and NH_3/NH_4^+. The fish were fed once or twice daily with Hikari tropical fancy guppy granulate (Hikari) and occasionally with spirulina flakes (Tropical). The tank was enriched with a natural gravel substrate, black sponge filters, and a turbine to generate water flow.

Eggs were collected from mass spawning events (two 1.7 L sloping breeding tanks were placed inside the in the maintenance tanks), rinsed in E3 medium (standard medium used for zebrafish, Cold Spring Harbor Protocols, https://cshprotocols.cshlp.org/content/2011/10/pdb.rec66449), and subjected to a quality check. Only clutches with at least 80% fertilized, healthy embryos were selected.

Experiments on zebrafish embryos and larvae up to 96 h post-fertilization (hpf) were conducted in compliance with European Union Directive 2010/63/EU and corresponding national regulations, which classify these developmental stages as non-protected due to their incapacity for independent feeding. Consequently, the experiment did not require prior approval from an ethics committee. All methods were carried out in compliance with the ARRIVE guidelines and relevant regulations and standards.

Due to limited enzyme availability, the standard acute fish embryo toxicity test (OECD No. 236[62]), was slightly modified. Groups of 12 embryos were placed in 3 cm diameter Petri dishes containing 2 mL of E3 medium. Before embryos reached the blastula stage, E3 was replaced with either 0 nM or 1000 nM solutions of StM23_CWT in E3. Embryos were incubated at 28 °C for four days, with daily checks for malformations, removal of dead embryos, and re-freshing of the medium. At the end of the experiment, embryos were assessed for survival and developmental abnormalities. Subsequently, they were euthanized by overdose of tricaine, following established protocols to ensure minimal distress.

Acute toxicity – invertebrate model

Final instar stage of the greater wax moth (*Galleria mellonella*) were obtained from a local supplier and stored in wood shavings at 8 °C in the dark for up to two weeks. One day prior to the experiment, larvae were acclimated to room temperature, transferred to 9 cm Petri dishes lined with a ring of paper towel, and kept overnight at room temperature in the dark. On the experiment day, batches containing at least 80% healthy, pigment-free larvae longer than 1.5 cm were selected. For the tests, groups of 10 larvae were used per treatment, with experiments repeated at least twice. Experimental groups were injected with 20 ± 2 µL of 1000 nM StM23_CWT in E3 medium through the last pro-leg using a 0.3 × 8 mm Micro-Fine Plus syringe (BD). Control groups included untreated larvae, larvae punctured with a needle, and larvae injected with the solvent (E3 medium). All larvae were maintained at 28 °C in the dark for up to 7 days, with daily monitoring for mortality. Larvae were classified as dead if melanization was observed or if they exhibited no movement upon gentle touch with forceps was observed. To assess mortality of later stages, cocoons and pupas were cut in half at the end of the experiments, and *G. mellonella* exhibiting dark, watery tissue were counted as dead.

Human cells viability - MTT assay

NIH 3T3 mouse fibroblasts (American Type Culture Collection; CRL-1658) and HaCAT human keratinocytes (Cell Line Service in Germany; 300493) were cultured in Dulbecco's Modified Eagle Medium (DMEM; Gibco, 11965-092) supplemented with 10% fetal bovine serum (FBS; Gibco A5256701) and 1% Penicillin-Streptomycin (PenStrep; Sigma, P0781-50 ml). When the cells reached approximately 80% confluency, they were washed with Dulbecco's Phosphate Buffered Saline (PBS; Sigma, D8537-500ML) and detached using TrypLE Express (Gibco, 12604-013). Cells were resuspended in antibiotic and phenol red-free DMEM (Gibco, 21063-029) supplemented with 10% FBS. Cell density was measured using a benchtop cell counter (Countess™, Invitrogen) and adjusted to 1×10^5 cells in milliliter. The cells (100 µL) were then seeded into 96-well plates (NEST, non-pyrogenic polystyrene) and incubated at 37 °C with 5% CO2 (Memmert incubator). For control wells, equal volume of medium without cells was added. After 24 h, the medium was replaced with fresh, filtered medium (0.22 µm filter, Millex-GV, Merck Millipore) with or without StM23_CWT and cells were incubated for additional 22–24-hour. Next, 10 µL of thiazolyl blue tetrazolium bromide (MTT; POL-AURA) solution was added to each well at a final concentration of 0.5 mg/mL and the plates with cells were incubated for 3 h at 37 °C. The formazan crystals which formed during this 3-hour incubation time were dissolved in dimethyl sulfoxide (DMSO; POL-AURA). To avoid any loss of crystals, 100 µL of DMSO was added directly into the wells with media and plates were left for 15–45 min with slow agitation. The quantity of formazan was measured by reading the absorbance at 570 nm using microplate photometer (Multiscan FC, ThermoScientific), and results were expressed as a percentage of viable cells relative to the untreated control group (set at 100%).

Statistical analysis

Data analysis was carried out using GraphPad Prism software version 10.0.3. A one-way and two-way ANOVA with post-hoc Tukey or Dunnett tests were applied to identify statistical difference between the samples. All

experiments were performed at least three times and data were presented as mean ± SD. The differences were considered significant at $P < 0.05$.

Data availability

Crystallographic data for this work was deposited in RCSB Protein Data Bank database under the PDB ID: 9GY1. All other study data are included within the manuscript.

Received: 15 January 2025; Accepted: 17 April 2025
Published online: 05 May 2025

References

1. Koopmans, M. M., Brouwer, M. C., Vázquez-Boland, J. A. & Van De Beek, D. Human listeriosis. *Clin. Microbiol. Rev.* **36**, e00060–e00019. https://doi.org/10.1128/cmr.00060-19 (2023).
2. Zwirzitz, B. et al. Co-Occurrence of Listeria spp. And spoilage associated microbiota during meat processing due to Cross-Contamination events. *Front. Microbiol.* **12**, 632935. https://doi.org/10.3389/fmicb.2021.632935 (2021).
3. Jarvis, N. A., Crandall, P. G., O'Bryan, C. A. & Ricke, S. C. Antimicrobial resistance in Listeria spp. In *Antimicrobial Resistance and Food Safety*. 137–153. https://doi.org/10.1016/B978-0-12-801214-7.00008-9. (Elsevier, 2015).
4. Wu, J., Wang, C. & O'Byrne, C. Metabolic reprogramming in the food-borne pathogen *Listeria monocytogenes* as a critical defence against acid stress. *FEMS Microbiol. Lett.* **371**, fnae060. https://doi.org/10.1093/femsle/fnae060 (2024).
5. Roedel, A. et al. Biocide-Tolerant Listeria monocytogenes isolates from German food production plants do not show Cross-Resistance to clinically relevant antibiotics. *Appl. Environ. Microbiol.* **85**, e01253–e01219. https://doi.org/10.1128/AEM.01253-19 (2019).
6. Møretrø, T. et al. Tolerance to quaternary ammonium compound disinfectants May enhance growth of Listeria monocytogenes in the food industry. *Int. J. Food Microbiol.* **241**, 215–224. https://doi.org/10.1016/j.ijfoodmicro.2016.10.025 (2017).
7. Mazaheri, T., Cervantes-Huamán, B. R. H., Bermúdez-Capdevila, M., Ripolles-Avila, C. & Rodríguez-Jerez, J. J. Listeria monocytogenes biofilms in the food industry: is the current hygiene program sufficient to combat the persistence of the pathogen?? *Microorganisms* **9**, 181. https://doi.org/10.3390/microorganisms9010181 (2021).
8. Fagerlund, A., Heir, E., Møretrø, T. & Langsrud, S. Listeria Monocytogenes biofilm removal using different commercial cleaning agents. *Molecules* **25**, 792. https://doi.org/10.3390/molecules25040792 (2020).
9. European Food Safety Authority (EFSA), European Centre for Disease Prevention and Control (ECDC). *The European Union One Health 2022 Zoonoses Report, EFS2 21*. (2023). https://doi.org/10.2903/j.efsa.2023.8442
10. Rippa, A. et al. Antimicrobial resistance of Listeria monocytogenes strains isolated in food and food-Processing environments in Italy. *Antibiotics* **13**, 525. https://doi.org/10.3390/antibiotics13060525 (2024).
11. Luque-Sastre, L. et al. Antimicrobial resistance in *Listeria* species. *Microbiol. Spectr.* **6**, 6.4.19. https://doi.org/10.1128/microbiolspec.ARBA-0031-2017 (2018).
12. Gray, J. A. et al. Novel biocontrol methods for Listeria monocytogenes biofilms in food production facilities. *Front. Microbiol.* **9**, 605. https://doi.org/10.3389/fmicb.2018.00605 (2018).
13. Loessner, M. J. Bacteriophage endolysins — current state of research and applications. *Curr. Opin. Microbiol.* **8**, 480–487. https://doi.org/10.1016/j.mib.2005.06.002 (2005).
14. Vermassen, A. et al. Cell wall hydrolases in bacteria: insight on the diversity of cell wall amidases, glycosidases and peptidases toward peptidoglycan. *Front. Microbiol.* **10**, 331. https://doi.org/10.3389/fmicb.2019.00331 (2019).
15. São-José, C. Engineering of Phage-Derived lytic enzymes: improving their potential as antimicrobials. *Antibiotics* **7**, 29. https://doi.org/10.3390/antibiotics7020029 (2018).
16. Eichenseher, F. et al. Linker-Improved chimeric endolysin selectively kills Staphylococcus aureus in vitro, on reconstituted human epidermis, and in a murine model of skin infection. *Antimicrob. Agents Chemother.* e0227321. https://doi.org/10.1128/aac.02273-21 (2022).
17. Jagielska, E., Chojnacka, O. & Sabała, I. LytM fusion with SH3b-Like domain expands its activity to physiological conditions. *Microb. Drug Resist.* **22**, 461–469. https://doi.org/10.1089/mdr.2016.0053 (2016).
18. Mitkowski, P., Jagielska, E. & Sabała, I. Engineering of chimeric enzymes with expanded tolerance to ionic strength. *Microbiol. Spectr.* **12**, e03546–e03523. https://doi.org/10.1128/spectrum.03546-23 (2024).
19. Nazir, A., Xu, X., Liu, Y. & Chen, Y. Phage endolysins: advances in the world of food safety. *Cells* **12**, 2169. https://doi.org/10.3390/cells12172169 (2023).
20. Schmelcher, M. & Loessner, M. J. Bacteriophage endolysins: applications for food safety. *Curr. Opin. Biotechnol.* **37**, 76–87. https://doi.org/10.1016/j.copbio.2015.10.005 (2016).
21. Holle, M. J. & Miller, M. J. Lytic characterization and application of Listerial endolysins PlyP40 and PlyPSA in Queso fresco. *JDS Commun.* **2**, 47–50. https://doi.org/10.3168/jdsc.2020-0013 (2021).
22. Schmelcher, M., Tchang, V. S. & Loessner, M. J. Domain shuffling and module engineering of *Listeria* phage endolysins for enhanced lytic activity and binding affinity. *Microb. Biotechnol.* **4**, 651–662. https://doi.org/10.1111/j.1751-7915.2011.00263.x (2011).
23. Quevillon, E. et al. InterProScan: protein domains identifier. *Nucleic Acids Res.* **33**, W116–120. https://doi.org/10.1093/nar/gki442 (2005).
24. Sabala, I. et al. Crystal structure of the antimicrobial peptidase lysostaphin from Staphylococcus simulans. *FEBS J.* **281**, 4112–4122. https://doi.org/10.1111/febs.12929 (2014).
25. Firczuk, M., Mucha, A. & Bochtler, M. Crystal structures of active LytM. *J. Mol. Biol.* **354**, 578–590. https://doi.org/10.1016/j.jmb.2005.09.082 (2005).
26. Wysocka, A., Jagielska, E., Łężniak, Ł. & Sabała, I. Two new M23 peptidoglycan hydrolases with distinct net charge. *Front. Microbiol.* **12**, 719689. https://doi.org/10.3389/fmicb.2021.719689 (2021).
27. Wysocka, A., Łężniak, Ł., Jagielska, E. & Sabała, I. Electrostatic interaction with the bacterial cell envelope Tunes the lytic activity of two novel peptidoglycan hydrolases. *Microbiol. Spectr.* e0045522. https://doi.org/10.1128/spectrum.00455-22 (2022).
28. Hussain, M. & Dawson, C. Economic impact of food safety outbreaks on food businesses. *Foods* **2**, 585–589. https://doi.org/10.3390/foods2040585 (2013).
29. Karanth, S., Feng, S., Patra, D. & Pradhan, A. K. Linking microbial contamination to food spoilage and food waste: the role of smart packaging, spoilage risk assessments, and date labeling. *Front. Microbiol.* **14**, 1198124. https://doi.org/10.3389/fmicb.2023.1198124 (2023).
30. Giaouris, E. et al. Attachment and biofilm formation by foodborne bacteria in meat processing environments: causes, implications, role of bacterial interactions and control by alternative novel methods. *Meat Sci.* **97**, 298–309. https://doi.org/10.1016/j.meatsci.2013.05.023 (2014).

31. Fagerlund, A., Møretrø, T., Heir, E., Briandet, R. & Langsrud, S. Cleaning and disinfection of biofilms composed of Listeria monocytogenes and background microbiota from meat processing surfaces. *Appl. Environ. Microbiol.* **83**, e01046–e01017. https://doi.org/10.1128/AEM.01046-17 (2017).
32. Rawlings, N. D., Waller, M., Barrett, A. J. & Bateman, A. MEROPS: the database of proteolytic enzymes, their substrates and inhibitors. *Nucleic Acids Res.* **42**, D503–509. https://doi.org/10.1093/nar/gkt953 (2014).
33. Razew, A., Schwarz, J. N., Mitkowski, P., Sabala, I. & Kaus-Drobek, M. One fold, many functions—M23 family of peptidoglycan hydrolases. *Front. Microbiol.* **13**. https://www.frontiersin.org/articles/. https://doi.org/10.3389/fmicb.2022.1036964 (2022). Accessed 28 Dec 2022.
34. Jayakumar, J., Kumar, V. A., Biswas, L. & Biswas, R. Therapeutic applications of lysostaphin against Staphylococcus aureus. *J. Appl. Microbiol.* **131**, 1072–1082. https://doi.org/10.1111/jam.14985 (2021).
35. Abaev, I. et al. Staphylococcal phage 2638A endolysin is lytic for Staphylococcus aureus and harbors an inter-lytic-domain secondary translational start site. *Appl. Microbiol. Biotechnol.* **97**, 3449–3456. https://doi.org/10.1007/s00253-012-4252-4 (2013).
36. Møretrø, T. & Langsrud, S. *Listeria monocytogenes*: biofilm formation and persistence in food-processing environments. *Biofilms* **1**, 107–121. https://doi.org/10.1017/S1479050504001322 (2004).
37. EFSA Panel on Biological Hazards (BIOHAZ). Evaluation of the safety and efficacy of listex™ P100 for reduction of pathogens on different ready-to-eat (RTE) food products. *EFS2 14*. https://doi.org/10.2903/j.efsa.2016.4565 (2016).
38. Kasra-Kermanshahi, R. & Mobarak-Qamsari, E. *Inhibition Effect of Lactic Acid Bacteria Against Food Born Pathogen, Listeria monocytogenes*. Vol. 2 (2015).
39. Castellano, P. et al. Antilisterial efficacy of Lactobacillus bacteriocins and organic acids on frankfurters. Impact on sensory characteristics. *J. Food Sci. Technol.* **55**, 689–697. https://doi.org/10.1007/s13197-017-2979-8 (2018).
40. Field, D., Fernandez de Ullivarri, M., Ross, R. P. & Hill, C. After a century of Nisin research - where are we now? *FEMS Microbiol. Rev.* **47**, fuad023. https://doi.org/10.1093/femsre/fuad023 (2023).
41. Gharsallaoui, A., Oulahal, N., Joly, C. & Degraeve, P. Nisin as a food preservative: part 1: physicochemical properties, antimicrobial activity, and main uses. *Crit. Rev. Food Sci. Nutr.* **56**, 1262–1274. https://doi.org/10.1080/10408398.2013.763765 (2016).
42. Ibarra-Sánchez, L. A., El-Haddad, N., Mahmoud, D., Miller, M. J. & Karam, L. Invited review: advances in Nisin use for preservation of dairy products. *J. Dairy Sci.* **103**, 2041–2052. https://doi.org/10.3168/jds.2019-17498 (2020).
43. Wu, J. et al. Nisin: from a structural and meat preservation perspective. *Food Microbiol.* **111**, 104207. https://doi.org/10.1016/j.fm.2022.104207 (2023).
44. Rollema, H. S., Kuipers, O. P., Both, P., De Vos, W. M. & Siezen, R. J. Improvement of solubility and stability of the antimicrobial peptide Nisin by protein engineering. *Appl. Environ. Microbiol.* **61**, 2873–2878. https://doi.org/10.1128/aem.61.8.2873-2878.1995 (1995).
45. Kumariya, R. et al. Bacteriocins: classification, synthesis, mechanism of action and resistance development in food spoilage causing bacteria. *Microb. Pathog.* **128**, 171–177. https://doi.org/10.1016/j.micpath.2019.01.002 (2019).
46. Jaskulski, I. B. et al. Listeria monocytogenes from food and food industry environments with reduced susceptibility to Benzalkonium chloride, sodium hypochlorite, and peracetic acid. *FEMS Microbiol. Lett.* **370**, fnad019. https://doi.org/10.1093/femsle/fnad019 (2023).
47. Rolon, M. L., Voloshchuk, O., Bartlett, K. V., LaBorde, L. F. & Kovac, J. Multi-species biofilms of environmental microbiota isolated from fruit packing facilities promoted tolerance of Listeria monocytogenes to Benzalkonium chloride. *Biofilm* **7**, 100177. https://doi.org/10.1016/j.bioflm.2024.100177 (2024).
48. Pennone, V. et al. Inhibition of *L. monocytogenes* biofilm formation by the amidase domain of the phage vB_LmoS_293 endolysin. *Viruses* **11**. https://doi.org/10.3390/v11080722 (2019).
49. Santativongchai, P. P., Tulayakul, P. P. & Jeon, B. Enhancement of the antibiofilm activity of Nisin against Listeria monocytogenes using food plant extracts. *Pathogens* **12**, 444. https://doi.org/10.3390/pathogens12030444 (2023).
50. Simmons, M., Morales, C. A., Oakley, B. B. & Seal, B. S. Recombinant expression of a putative amidase cloned from the genome of Listeria monocytogenes that lyses the bacterium and its monolayer in conjunction with a protease. *Probiotics Antimicro Prot.* **4**, 1–10. https://doi.org/10.1007/s12602-011-9084-5 (2012).
51. Tirloni, E. et al. Bacillus cereus in dairy products and production plants. *Foods* **11**, 2572. https://doi.org/10.3390/foods11172572 (2022).
52. Perdomo, A. & Calle, A. Assessment of microbial communities in a dairy farm from a food safety perspective. *Int. J. Food Microbiol.* **423**, 110827. https://doi.org/10.1016/j.ijfoodmicro.2024.110827 (2024).
53. Fernández-No, I. C. et al. Characterisation and profiling of Bacillus subtilis, Bacillus cereus and Bacillus licheniformis by MALDI-TOF mass fingerprinting. *Food Microbiol.* **33**, 235–242. https://doi.org/10.1016/j.fm.2012.09.022 (2013).
54. Møretrø, T. & Langsrud, S. Residential Bacteria on surfaces in the food industry and their implications for food safety and quality. *Comp. Rev. Food Sci. Food Safe.* **16**, 1022–1041. https://doi.org/10.1111/1541-4337.12283 (2017).
55. Klock, H. E. & Lesley, S. A. The polymerase incomplete primer extension (PIPE) method applied to High-Throughput cloning and Site-Directed mutagenesis, in: (ed Doyle, S. A.) High Throughput Protein Expression and Purification: Methods and Protocols, Humana, Totowa, NJ, : 91–103. https://doi.org/10.1007/978-1-59745-196-3_6. (2009).
56. Kabsch, W. XDS. *Acta Crystallogr. D Biol. Crystallogr.* **66**, 125–132. (2010). https://doi.org/10.1107/S0907444909047337
57. Krug, M., Weiss, M. S., Heinemann, U. & Mueller, U. XDSAPP: a graphical user interface for the convenient processing of diffraction data using XDS. *J. Appl. Cryst.* **45**, 568–572. https://doi.org/10.1107/S0021889812011715 (2012).
58. McCoy, A. J. et al. Phaser crystallographic software. *J. Appl. Crystallogr.* **40**, 658–674. https://doi.org/10.1107/S0021889807021206 (2007).
59. Afonine, P. V. et al. Towards automated crystallographic structure refinement with phenix.refine. *Acta Cryst. D.* **68**, 352–367. https://doi.org/10.1107/S0907444912001308 (2012).
60. Emsley, P. & Cowtan, K. Coot: model-building tools for molecular graphics. *Acta Crystallogr. D Biol. Crystallogr.* **60**, 2126–2132. https://doi.org/10.1107/S0907444904019158 (2004).
61. Hartmann, M. et al. Damage of the bacterial cell envelope by antimicrobial peptides Gramicidin S and PGLa as revealed by transmission and scanning Electron microscopy. *Antimicrob. Agents Chemother.* **54**, 3132–3142. https://doi.org/10.1128/AAC.00124-10 (2010).
62. OECD Guidelines for the Testing of Chemicals. *Test No. 236: Fish Embryo Acute Toxicity (FET) Test, OECD Guidelines for the Testing of Chemicals, Section 2* (OECD Publishing, 2013). https://doi.org/10.1787/9789264203709-en

Acknowledgements

The authors express their gratitude to Ryszard Strzalkowski for preparing and visualizing samples using scanning electron microscopy, and to Grazyna Madejska and Joanna Kruss for preparing samples for transmission electron microscopy. We also thank the Kuznicki lab at the International Institute of Molecular and Cell Biology in Warsaw for providing NIH 3T3 fibroblasts, and Wiesława Leśniak from the Nencki Institute of Experimental Biology in Warsaw for providing HaCAT keratinocytes.

Author contributions

M. K-D. designed, performed experiments, analyzed data, prepared Figs. 2, 3 and 4, wrote the main manuscript. M.N. helped with structure determination and prepared figure 1. M.G. did electron microscopy studies, prepared figure 5 and wrote section about electron microscopy. M.K. did safety evaluation studies, prepared figure 6 and wrote section about safety studies. M.R., T.M. and E.H. did biofilms studies, wrote section results with biofilm eradication. E.N. helped with structure determination. I.S. obtained funding, administrated project and supervised. All authors reviewed the manuscript.

Funding

This work was supported by the National Centre for Research and Development supported by Norway grants in POLNOR2019 "Applied Research" program [NOR/POLNOR/PrevEco/0021/2019 and (NOR/POLNOR/SafeFoodCtrl/0034/2019)] Funding to complete the work for scientific publication was also obtained from the Norwegian Fund for Research Fees for Agricultural Products (FFL), grant no. 314,743. IIMCB core facilities (INMOL-CELL infrastructure) were funded by the European Union and co-financed under the European Funds for Smart Economy 2021–2027 (FENG).

Declarations

Competing interests

Magdalena Kaus-Drobek, Marzena Nowacka and Izabela Sabala are authors of a patent application filed with the Polish Patent Office (ID: ZP.261.018.2024.017), entitled "Recombinant peptidoglycan hydrolase protein with antibacterial properties, compositions containing it, their applications, and methods of use". Izabela Sabała is an Editorial Board Member in Scientific Reports in Structural and Molecular Biology section.

Additional information

Supplementary Information The online version contains supplementary material available at https://doi.org/10.1038/s41598-025-99141-2.

Correspondence and requests for materials should be addressed to M.K.-D. or I.S.